Pyridine Containing 1,2,4 Triazole Derivatives as a Potent Inhibitor of JNK Pathway for Prevention of Tumorigenesis in Breast and Hepatocellular

Section A-Research paper

Pyridine Containing 1,2,4 Triazole Derivatives as a Potent Inhibitor of JNK Pathway for Prevention of Tumorigenesis in Breast and Hepatocellular

Priyanka A. Patil*[1,2], Preeti Khulbe[1], Ashwini C Utage[2], Gayatri S Jagtap[3]

[1]School of Pharmacy, Suresh Gyan Vihar University, Jaipur, Rajasthan, India 302017.
[2]Dr. Shivajirao Kadam College of Pharmacy, Kasabe Digraj, Sangli, Maharshtra, India 415305
[3]Shree Santkrupa College of Pharmacy, Ghogaon, Satara Maharshtra, India **415111.**
(papatil8001@gmail.com, preeti.khulbe@mygyanvihar.com, ashwiniutage1992@gmail.com, gayatrijagtap851@gmail.com)

Corresponding author: Name: Priyanka A. Patil, Email Id: papatil8001@gmail.com
Orcid Id: 0000-0002-4474-1754

Abstract: A series of some new Triazole derivatives was synthesized from substituted aryl isocyanate. Synthesized compounds were characterized through infrared, proton nuclear magnetic resonance, and Mass spectroscopy. The synthesized derivatives were evaluated in vitro for their cytotoxic activity against MCF-7 cell lines. The compound AM 4B exhibited a strong cytotoxic effect against MCF -7 with IC 50 of of 29.39 µg/mol. Furthermore, toxicity and ADMET calculations were performed for the synthesized compounds to study their pharmacokinetic profiles.

Introduction

With ongoing attempts to assess its biochemistry, regulation, and contribution to cellular processes under physiological and pathological situations, the c-Jun N-terminal kinase family (JNK) has continued to be a topic of great study interest. One of the three families of mitogen-activated protein (MAP) kinases that have been found is the JNK family of protein kinases. JNK1 (MAPK8), JNK2 (MAPK9), and JNK3 (MAPK3) are three genes (MAPK10) [1].

 A wide range of human tissues express JNK1 and JNK2 always. JNK1 and JNK2 [4] have been linked to the emergence of diabetes, obesity, arthritis, cancer, and heart disease, according to recent studies[2,5]. JNK1 appears to contribute to the onset of obesity-induced insulin resistance, suggesting that inhibiting JNK1 may be a useful treatment for type 2 diabetes [6,7]. Numerous autoimmune illnesses, including rheumatoid arthritis, asthma, and cancer, as well as a wide spectrum of conditions with an inflammatory component, have been linked to JNK2 [5,8]. JNK3 has a significant role in Alzheimer's disease [9], Parkinson's disease, and stroke and is largely expressed in the central nervous system (CNS) [3,10,11]. Therefore, the development of JNK inhibitors as therapeutic drugs has attracted a great deal of interest during the past several years. JNK inhibitors may have significance in many therapeutic domains [12-17].

Experimental: Instruments and Materials:

Solvents and other reagents were employed in the synthesis of the target compounds in this work. These ingredients were provided by commercial vendors and used without additional purification. On 0.25 mm silica gel plates (60GF-254), reactions were observed by thin-layer chromatography

Eur. Chem. Bull. **2022**,11(issue 10), 243-252

243

(TLC) and observed under UV light (254 or 365 nmol/L). The Infra-red Spectroscopy were obtained on Jasco FTIR 4600. Tetramethylsilane (TMS) was used as the standard to measure the 1H nuclear magnetic resonance (NMR) spectra on a Brucker spectrometer (400 MHz or 300 MHz) at 25 °C. The chemical shifts are reported relative to the solvent line, which serves as the internal standard, and are expressed as values (parts per million). The following order in which splitting patterns were displayed: A multiplet m, singlet s, a doublet d or a triplet t. Mass spectrometer (MS) spectra were acquired on an Agilent G 6160.

General method for synthesis of arylhydrazine carbothioamide: 18-19
A mixture of aryl-3-carbohydrazide 1 (0.01 mol) and the properly substituted phenyl isothiocyanate (0.01 mol) was heated under reflux for 6 hours in 40 mL of ethanol. The reaction mixture was cooled, the resulting solid was filtered, diethyl ether washed to remove any remaining isothiocyanate, water washed to remove any remaining hydrazine, dried, and crystallised from the ethanol.

General method for synthesis of substituted aryl-1,2,4-Triazol:
A solution of the appropriate carbothioamide AM1A–AM1E (0.01 mol) in 1 N NaOH (30 mL) was heated under reflux for 2 h. The solution was cooled and acidified to pH 5–6 with acetic acid. The precipitate formed was filtered, washed with water and crystallized from solvent.

Scheme

AM 4A - AM 4E
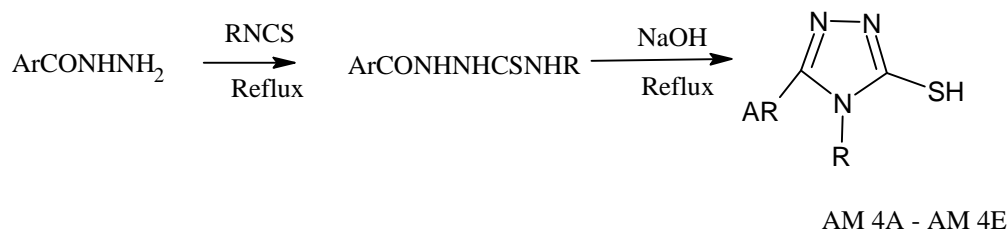
4-phenyl-5-(pyridin-3-yl)-4*H*-1,2,4-triazole-3-thiol (AM 4A)
% Yield: 85%; melting point: 265-268°C; IR (cm−1): 3096 (NH), 2916 (aromatic CH), 2360 (SH), 1593(C=N), 1326 (C=S); 1H-NMR (500 MHz, DMSO) δ: 8.58 (d, 1H pyridine H-2), 8.49 (dd, 1H, pyridine H-6), 7.67 (m,1H pyridine H- 4), 7.52 (m,1H pyridine H- 5), 7.36–7.51(m, 5H, Ar-H);   *m/z* (%) 255.0 (M+1).

4-(3-chlorophenyl)-5-(pyridin-3-yl)-4*H*-1,2,4-triazole-3-thiol (AM 4B)
% Yield: 67%; melting point: 250-254°C; IR (cm−1): 3357 (NH), 2916 (aromatic CH), 2359 (SH), 1589(C=N), 1397(C=S), 770 (C-Cl); 1H-NMR (500 MHz, DMSO) δ: 8.87 (d, 1H pyridine H-2), 8.56 (dd, 1H, pyridine H-6), 8.25 (m,1H pyridine H- 4), 7.63 (m,1H pyridine H- 5), 7.30–7.57 (m, 4H, Ar-H);   *m/z* (%) 289.2 (M+1).

4-benzyl-5-(pyridin-3-yl)-4*H*-1,2,4-triazole-3-thiol (AM 4C)

% Yield: 73%; melting point: 278-280°C; IR (cm−1): 3109 (NH), 2914 (aromatic CH), 2360 (SH), 1515 (C=N), 1343(C=S); 1H-NMR (500 MHz, DMSO) δ: 8.69 (d, 2H pyridine H-2, H-6), 7.96 (d,1H pyridine H- 4), 7.50 (m,1H pyridine H- 5), 5.39(M, 1H, CH) 7.00–7.27 (m, 4H, Ar-H); *m/z* (%) 269.2 (M+1).

4-(4-fluorophenyl)-5-(pyridin-3-yl)-4*H*-1,2,4-triazole-3-thiol (AM 4D)

% Yield: 78%; melting point: 240-242°C; IR (cm−1): 3115 (NH), 3035 (aromatic CH), 2681 (SH), 1509 (C=N), 1331 (C=S), 1027 (C-F); 1H-NMR (500 MHz, DMSO) δ: 8.61 (d, 1H pyridine H-2), 8.53 (dd, 1H, pyridine H-6), 7.66 (m,1H pyridine H- 4), 7.49 (m,2H pyridine H- 5, 1H Ar), 7.33–7.49 (m, 3H, Ar-H); *m/z* (%) 273.1 (M+1).

4-(4-nitrophenyl)-5-(pyridin-3-yl)-4*H*-1,2,4-triazole-3-thiol (AM 4E)

% Yield: 55%; melting point: 232-235°C; IR (cm−1): 3324 (NH), 2916 (aromatic CH), 2360 (SH), 1590 (C=N), 1249 (C=S), 1497 (N-O); 1H-NMR (500 MHz, DMSO) δ: 8.02 (m, 2H pyridine H-2, H-6), 7.87 (m, 2H, pyridine H-4, H- 5), 5.83–7.6.60 (m, 4H, Ar-H); *m/z* (%) 300.2 (M+1).

Biological Evaluation

Antiproliferative Activity: 20

Using the MTT assay, the antiproliferative properties of all the synthesized triazole derivatives were evaluated against the MCF-7, breast cancer cell line. In a nutshell, MCF-7 cells were grown in RPMI1640 media with 10% FBS for 24 hours before being exposed to drugs. The cells were then plated with per cell 4,000–5,000 into 96-well plates for MCF-7 cells. The synthesized compounds were weighed and dissolved in DMSO, then diluted to the required quantities. The test chemicals were applied to cells at final concentrations of 100, 40, and 10μg/mL and incubated for 24 hours. Then, 20 μL of each well received a concurrent addition of 0.5% MTT solution, which was then incubated for 4 hours at 37 °C. DMSO (150 L) was poured into solution which dissolves the crystal of formazan. The absorbance of each sample was measured using a microplate reader (Benesphera E21) at a wavelength of 550 nm to evaluate the triplicate samples. The inhibition ratios were used to determine the IC50 value.

The following equations was applied to assess the cell viability:

% Viability = (optical density of sample/optical density of control) × 100

Result
In vitro Anticancer Screening:

By using MTT assay against the tumour cell lines MCF-7, all 1,2,4 triazole derivatives that had been produced were assessed for their in vitro antiproliferative properties. The findings showed that all compounds examined, AM4A- AM4E, had acceptable antiproliferative properties for specific tumour cell lines.

The results were reported IC 50 value in **Table 1.** Among the five triazoles screened for cytotoxicity in MTT assay against MCF-7 cell line, AM 4B exhibited excellent cytotoxicity with IC50 values of 29.39 µg/mL. The halogen group in the phenyl ring probably might have augmented the activity of AM 4B. The IC50 for the standard drug 5 FU was found to be 52.61 µg/mL.

Antiproliferative Activity:

Table 1: Cytotoxicity of Compounds AM 4A – AM 4E against a Variety of Cancer Cell Lines [IC50(µg/ml)]

IC50 Values (µg/ml)	
Compound	**IC50 MCF -7**
5 FU	52.61
AM 4A	54.12
AM 4B	29.39
AM 4C	63.53
AM 4D	41.3
AM 4E	57.45

In silico Prediction of absorption distribution metabolism and elimination (ADME) properties and drug-likeness [21-23].

To estimate the properties of absorption, distribution, metabolism, and elimination (ADME), computational research of titled substances was conducted. Using the SWISS ADME online web tool and the Molinspiration online property calculation tool set, researchers were able to compute the total polar surface area (TPSA), Log P, the number of rotatable bonds, molecular volume, and the number of hydrogen donor and acceptor atoms. Drug design utilizes the qualitative idea of drug-likeness. The Lipinski Rule of Five [24], known as Pfizer's or Lipinski's rules, was described in 1997 by Christopher Lipinski which considers molecular weight, hydrophobicity, and the number of hydrophilic groups, must be followed to determine drug-likeness. A synthetic compound's drug-likeness features were evaluated using the SWISS ADME Web tool.

TPSA, drug likeness, and pharmacokinetic properties

A bioactive molecule's high oral bioavailability is crucial for the development of the molecule as a medicinal treatment. Important predictors of this feature are good intestine absorption, reduced molecule flexibility, low polar surface area, or total hydrogen bond count (some of the donors and some of the accepters) [25]. Any compound's bioactivity is generated and determined in large part by its physicochemical properties. A few fundamental molecular descriptors, such as the partition coefficient (log P), molecular weight (Mw), or the amount of hydrogen bond acceptors and donors in the molecule, are invariably associated with certain molecular features, such as membrane permeability and bioavailability [26].

According to the rule, the majority of molecules with strong membrane permeability have log P values of 5, Mw values of 500, ten hydrogen bond acceptors, and five hydrogen bond donors. This criterion is frequently applied as a screening for drug attributes. Another factor that can be used to describe the permeability of drugs is hydrogen bonding capability [27]. When the chemical possesses more than five H-bond donors and more than ten H-bond acceptors, poor penetration or absorption is more likely.

 In the present study, 1,2,4 Triazole derivatives have a number of H-bond acceptors ($\leq$ 10) and a lower number of hydrogen bond donors ($\leq$ 5) **(Table 2).** When it comes to conformational flexibility and binding acceptors or passageways, the quantity of rotatable bonds is crucial. The minimum allowed number of rotatable bonds for oral bioavailability is 10. The title compounds demonstrate significant conformational flexibility because they have a high number of rotate -ble bonds (0–5) [28].

An especially useful metric for predicting drug transport characteristics is the molecular polar surface area (PSA), which is the sum of the surfaces of polar atoms in a molecule (often oxygen, nitrogen, and associated hydrogen). Drug absorption, including stomach absorption, bioavailability, CaCO2 permeability, and bloodbrain barrier permeability, has been characterised by topological polar surface area (TPSA). (Table 3).

One straightforward topological parameter that assesses molecular flexibility is the number of rotatable bonds (nrotb).
Any single nonring bond that is bound to a nonterminal atom and is referred to as a rotatable bond has been demonstrated to be an excellent indicator of a drug's oral bioavailability. The drug likeness score was calculated by MolSoft and combined the effects of a compound's physicochemical characteristics, pharmacokinetics, and pharmacodynamics.
The Milog P (logarithm of the octanol/water partition coefficient), molecular weight, number of heavy atoms, number of hydrogen donors, number of hydrogen acceptors, number of violations, number of rotatable bonds, and volume were taken into account while calculating the drug similarity score. Based on GPCR ligand (GPCRL), ion channel modulator (ICM), nuclear receptor legend (NRL), and kinase inhibitor bioactivity scores, isolated substances are compared to conventional drugs**. (Table 4).**

Boiled EGG PLOT analysis
Besides ADMET, effectiveness, and toxicity, weak bioavailability and pharmacokinetics are the outcomes of drug development failures. The two most important pharmacokinetic activities that must be evaluated at various stages of the drug discovery procedures are gastrointestinal absorption and brain access. Here, the Physicochemical properties of tiny compounds, such as polarity and lipophilicity, are estimated using the Brain or IntestinaL EstimateD permeation technique (BOILEDEgg) permeation predictive model diagram, including passive human gastrointestinal absorption (HIA), blood–brain barrier (BBB) permeation. The analysis explains that a high BBB crossing is possible when the established compound pitching occurs inside the yellow ellipse or the yolk. The best virtual screened molecule, on the other hand, pitches inside the white ellipse, indicating the potential for significant intestine absorption Figure 1. [29-30].

Intuitive analysis of the examined substances' bioavailability radars is possible (Figure 2).
The druglikeness graphs, which are specific to SwissADME, are presented in the shape of hexagons, with each vertex denoting a characteristic that characterises a bioavailable medication. Lipophilicity (XLOGP3 between 0.7 and +5.0), size (MW between 150 and 500), polarity (TPSA between 20 and 130 A^0), solubility (log S not higher than 6), saturation (fraction of carbons in the sp3 hybridization not less than 0.25) and flexibility are the six properties that fall within the ideal ra

nge shown by the pink regions (no more than nine rotatable bonds). The pink tone has a red disto rted hexagon, which stands for drug-like qualities.

In silico Pharmacokinetic and Toxicity Prediction:

AdmetSAR software was used to estimate various ADMET properties of the best-established compound. The compounds were submitted in SMILES file format for the computation. The AMES toxicity test determines a substance's mutagenicity. In the case of the established compound, a negative AMES toxicity test result was designated by the processed ligand compound which indicates that the compound is non-mutagenic. Also, the virtual screened compound is noncarcinogenic and it is showing a lower value. Here compounds GI absorption and oral bioavailability were predicted [31]. The toxicity study was performed using the Admet SAR online server, which predicted that all derivatives were not mutagenic and neither were they carcinogenic, rendering these acceptable for biological usage. In **Table 5,** the results of the toxicity prediction computation were compiled. All derivatives have about the same acute toxicity in rats as standard.

Table 2: Lipinski parameters with absorption distribution metabolism elimination properties and Drug likeness properties of synthesized 1,2,4 Triazole derivatives.

Physicochemical Properties							Drug Likness				
Compound	Mol. wt	H-accepter	H-donor	Rotatable bond	Log *p*	Total polar surface area (TPSA)	Lipinski violations	Ghose violations	Veber violations	Bioavaiability Score	Synthetic Accessibility
AM 4A	254.31	2	1	2	2.04	78.59	0	0	0	0.55	2.36
AM 4B	288.76	2	1	2	2.23	78.59	0	0	0	0.55	2.49
AM 4C	268.34	2	1	3	2	78.59	0	0	0	0.55	2.34
AM 4D	272.3	3	1	2	2.12	78.59	0	0	0	0.55	2.34
AM 4E	299.31	4	1	3	1.62	124.41	0	0	0	0.55	2.55

Table 3: Pharmacokinetic Prediction of synthesized 1,2,4 Triazole derivatives using SWISS ADME

Compound	GI Absorption	Caco absorption	p-gp	CYP1A2 inhibitor	CYP2C19 Inhibitor	CYP2D6 Inhibitor
AM 4A	High	Yes	No	Yes	Yes	No
AM 4B	High	Yes	No	Yes	Yes	No
AM 4C	High	Yes	No	Yes	Yes	No
AM 4D	High	Yes	No	Yes	Yes	No
AM 4E	High	Yes	No	Yes	Yes	No

Table 4: Molinspiration Bioactivity Score of synthesized 1,2,4 Triazole derivatives

Compound	GPCR ligand	Ion channel modulator	Kinase Inhibitor	Nuclear receptor ligand	Protease inhibitor	Enzyme inhibitor

AM 4A	-0.69	-0.60	-0.79	-1.19	-1.03	-0.58
AM 4B	-0.64	-0.60	-0.75	-1.09	-1.03	-0.60
AM 4C	-0.53	-0.68	-0.68	-0.84	-0.76	-0.34
AM 4D	-0.60	-0.58	-0.66	-1.04	-0.96	-0.55
AM 4E	-0.67	-0.59	-0.73	-1.01	-0.93	-0.61

**Table 5: Toxicity prediction by using Admet SAR online web tool of synthesized 1,2,4 Triazole derivatives.**

Sr No	Compound	Ames Mutagenesis	Carcinogen	Acute Oral Toxicity	Acute Toxicity LD50 mol/Kg
1.	AM 4A	0.6900	0.8500	III 0.7258	2.611
2.	AM 4B	0.7400	0.7919	III 0.7024	2.368
3.	AM 4C	0.6600	0.7800	III 0.6739	2.79
4.	AM 4D	0.6200	0.8219	III 0.6889	2.406
5.	AM 4E	0.7900	0.8300	III 0.5677	2.392

Based on the obtained computational ADME and toxicity data synthesized 1,2,4 Triazole derivatives compounds were chosen for *in-vitro* studies.
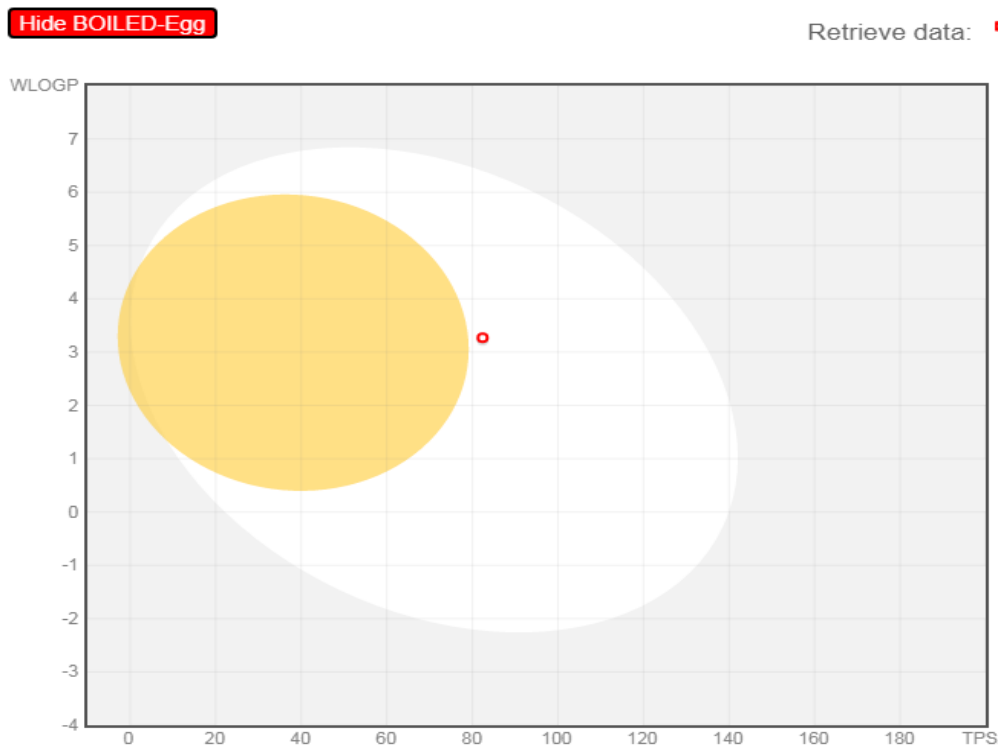
Figure 1: Boiled Egg Plot of most effective Virtual Screened and Established compound AM 4B.
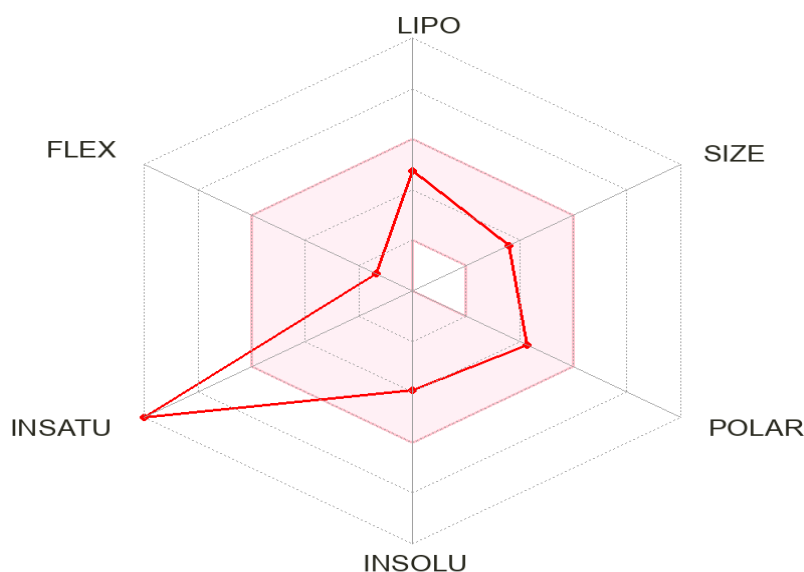
Figure 2: Shows the bioavailability radar of compound AM 4B (pink area exhibits optimal range of particular property) for the compounds under study: LIPO (lipophilicity as XLOGP3), SIZE (size as molecular weight), POLAR (polarity as TPSA), INSOLU (insolubility in water by log S scale), INSATU (insaturation as per fraction of carbons in the sp3 hybridization), and FLEX (flexibility as per rotatable bond).

Conclusion

The compounds were checked for lipinski's rule and veber rule as drug likeness parameters. All the compounds pass the lipinski rule of five, which guarantees that compounds will have higher binding affinity on target and good oral bioavaibility. The novel heterocyclic compounds were synthesized by conventional method with high yield and purity. All compounds were in conformity with the structure envisaged. The structures were proved on the basis of, IR, H1NMR and Mass spectroscopy. Among the ten triazoles screened for cytotoxicity in MTT assay against MCF-7 cell lines, AM 4B exhibited excellent cytotoxicity with IC50 values of 29.39 µg/mL. The halogen group in the phenyl ring probably might have augmented the activity of AM 4B.

References:

1. Davis, R. J. (2000). Signal transduction by the JNK group of MAP kinases. Cell 103, 239–252. doi: 10.1016/S0092-8674(00)00116-1
2. Gupta S.; Barrett T.; Whitmarsh A. J.; Cavanagh J.; Sluss H. K.; Derijard B.; Davis R. J. Selective interaction of JNK protein kinase isoforms with transcription factors. *EMBO J.* 1996, 15, 2760–2770.
3. Chambers J. W.; Howard S.; LoGrasso P. V. Blocking c-Jun N-terminal kinase (JNK) translocation to the mitochondria prevents 6-hydroxydopamine-induced toxicity in vitro and in vivo. *J. Biol. Chem.* 2013, 288, 1079–1088

4. Derijard B.; Hibi M.; Wu I. H.; Barrett T.; Su B.; Deng T. L.; Karin M.; Davis R. J. Jnk1 - a protein-kinase stimulated by UV-light and Ha-Ras that binds and phosphorylates the C-Jun activation domain. *Cell* 1994, 76, 1025–1037

5. Zhang H.; Shi X. Q.; Zhang Q. J.; Hampong M.; Paddon H.; Wahyuningsih D.; Pelech S. Nocodazole-induced p53-dependent c-Jun N-terminal kinase activation reduces apoptosis in human colon carcinoma HCT116 cells. *J. Biol. Chem.* 2002, 277, 43648–43658.

6. Chang L. F.; Jones Y.; Ellisman M. H.; Goldstein L. S. B.; Karin M. JNK1 is required for maintenance of neuronal microtubules and controls phosphorylation of microtubule-associated proteins. *Dev. Cell* 2003, 4, 521–533. [PubMed] [Google Scholar]

7. Hirosumi J.; Tuncman G.; et al S. A central role for JNK in obesity and insulin resistance. *Nature* 2002, 420, 333–336

8. Blease K.; Lewis A.; Raymon H. K. Emerging treatments for asthma. *Expert Opin. Emerg. Drugs* 2003, 8, 71–81. [PubMed] [Google Scholar]

9. Yoon S. O.; Park D. J.; Ryu J. C.; Ozer H. G.; Tep C.; Shin Y. J.; Lim T. H.; Pastorino L.; Kunwar A. J.; Walton J. C.; Nagahara A. H.; Lu K. P.; Nelson R. J.; Tuszynski M. H.; Huang K. JNK3 perpetuates metabolic stress induced by Abeta peptides. *Neuron* 2012, 75, 824–37. [PMC free article] [PubMed] [Google Scholar]

10. Chambers J. W.; Pachori A.; Howard S.; et.al. Small molecule c-jun-N-terminal kinase (JNK) inhibitors protect dopaminergic neurons in a model of Parkinson's disease. *ACS Chem. Neurosci.* 2011, 2, 198–206. [PMC free article] [PubMed] [Google Scholar]

11. Crocker C. E.; Khan S.; Cameron M. D.; Robertson H. A.; Robertson G. S.; LoGrasso P. JNK inhibition protects dopamine neurons and provides behavioral improvement in a rat 6-hydroxydopamine model of Parkinson's disease. *ACS Chem. Neurosci.* 2011, 2, 207–212. [PMC free article] [PubMed] [Google Scholar]

12. Cao J. R.; Gao H.; Bemis G.; Salituro F.; Ledeboer M.; Harrington E.; Wilke S.; Taslimi P.; Pazhanisamy S.; Xie X. L.; Jacobs M.; Green J. Structure-based design and parallel synthesis of N-benzyl isatin oximes as JNK3 MAP kinase inhibitors. *Bioorg. Med. Chem. Lett.* 2009, 19, 2891–2895. [PubMed] [Google Scholar]

13. He Y. J.; Kamenecka T. M.; Shin Y. S.; Song X. Y.; Jiang R.; Noel R.; Duckett D.; Chen W. M.; Ling Y. Y.; Cameron M. D.; Lin L.; Khan S.; Koenig M.; LoGrasso P. V. Synthesis and SAR of novel quinazolines as potent and brain-penetrant c-jun N-terminal kinase (JNK) Inhibitors. *Bioorg. Med. Chem. Lett.* 2011, 21, 1719–1723. [PMC free article] [PubMed] [Google Scholar]

14. Kamenecka T.; Habel J.; Duckett D.; Chen W. M.; Ling Y. Y.; Frackowiak B.; Jiang R.; Shin Y. S.; Song X. Y.; LoGrasso P. Structure-activity relationships and X-ray structures describing the selectivity of aminopyrazole inhibitors for c-Jun N-terminal kinase 3 (JNK3) over p38. *J. Biol. Chem.* 2009, 284, 12853–12861. [PMC free article] [PubMed] [Google Scholar]

15. Kamenecka T.; Jiang R.; Song X. Y.; Duckett D.; Chen W. M.; Ling Y. Y.; Habel J.; Laughlin J. D.; Chambers J.; Figuera-Losada M.; Cameron M. D.; Lin L.; Ruiz C. H.; LoGrasso P. V. Synthesis, biological evaluation, X-ray structure, and pharmacokinetics of aminopyrimidine c-jun-N-terminal kinase (JNK) inhibitors. *J. Med. Chem.* 2010, 53, 419–431. [PMC free article] [PubMed] [Google Scholar]

16. Krenitsky V. P.; Delgado M.; Nadolny L.; et. al. Aminopurine based JNK inhibitors for the prevention of ischemia reperfusion injury. *Bioorg. Med. Chem. Lett.* 2012, 22, 1427–1432. [PubMed] [Google Scholar]

17. Swahn B. M.; Xue Y.; Arzel E.; Kallin E.; Magnus A.; Plobeck N.; Viklund J. Design and synthesis of 2′-anilino-4,4′-bipyridines as selective inhibitors of c-Jun N-terminal kinase-3. *Bioorg. Med. Chem. Lett.* 2006, 16, 1397–401. [PubMed] [Google Scholar]

18. Mishra R. K., Tewari R. K. Synthesis and Antifungal Activity of some 1,4-Disubstituted-thiosemicarbazides, 2,5-Disubstituted-1,3,4-thiadiazoles and 3,4-Disubstituted-5-mercapto-1,2,4-triazoles *J. Indian Chem. Soc.,* 1991, 68, 110–113.

19. Priyanka Annaso Patil*, Preeti Khulbe, "Design, Synthesis and Biological evaluation of some New N-(Substituted Pyridine-3-yl)-1,3,4- Oxadiazol-2-Amines", Indian Journal of Heterocyclic Chemistry, Vol 33, Number 1 (Jan-March 2023) 71-78, ISSN: 0971-1627. DOI: 01951.2023.33.71

20. Shringare SN., Chavan HV., Bhale PS, Dongare S B, Mule YB, Patil SB, Bandgar BP. Synthesis and pharmacological evaluation of combretastatin-A4 analogs of pyrazoline and pyridine derivatives as anticancer, anti-inflammatory and antioxidant agents, Medicinal *Chemistry Research* 2018, 27 (4), 1226-1236, Springer Journals

21. Lipinski CA , Lombardo F , Dominy BW , Feeney PJ . 1997. Experimental and computational approaches to estimate solubility and permeability in drug discovery and development settings. Adv Drug Delivery Rev. 23:4–25.

22. Bhal SK, Kassam K, Peirson IG, Pearl GM. 2007. The rule of five revisited: applying Log D in place log p in drug likeness filters. Mol Pharma;4(4):556–60.

23. Molinspiration c heminformatics, Bratislava, Slovak Republic, a nd Avail- able from: http://www.molinspiration.com/services/properties.html ; [accessed 16.08.10] .

24. Lipinski CA, Lomardo F, et al. 2012. Experimental and computational approaches to estimate solubility and permeability in drug discovery and development settings. Adv Drug Deliv Rev. 64: 4-17. DOI: 10.1016/j.addr.2012.09.019.

25. Refsgaard, H.H.F., Jensen, B.F., Brockhoff, P.B., Padkjaer, Guldbrandt S.B., and Christensen, M.S.,In silico prediction of membrane permeability from calculated molecular parameters. J. Med. Chem., 2005; 48: 805-811. Doi 10.1021/jm049661n

26. Muegge, I., Selection Criteria for Drug-Like Compounds Med. Res. Rev*.,* 2003; 23: 302-321. Doi 10.1002/med.10041

27. Veber D.F., Johnson, S.R., Cheng, H.Y., Smith, B.R.,Ward, K.W., and Kapple, K.D.,Molecular properties that influence the oral bioavailability of drug candidates. J. Med. Chem., 2002; 45: 2615-2623. doi 10.1021/jm020017n

28. Joanna Bojarska , Milan Remko , Martin Breza et al. A Supramolecular Approach to Structure-Based Design with A Focus on Synthons Hierarchy in Ornithine-Derived Ligands: Review, Synthesis, Experimental and in Silico Studies. Molecules 2020;25: 1135-1162; doi:10.3390/molecules25051135

29. Daina A, Zoete V. A boiled-egg to predict gastrointestinal absorption and brain penetration of small molecules. Chem Med Chem 2016;11(11):1117–1121.

30. Daina A, Michielin O, Zoete V. Swiss ADME: a free web tool to evaluate pharmacokinetics, drug-likeness and medicinal chemistry friendliness of small molecules. Sci Rep 2017;7(1):1–13

31. Amin ML..P-glycoprotein inhibition for optimal drug delivery. Drug Target Insights. 2013;19(7):27-34. doi: 10.4137/DTI.S12519.